APPLIED AND ENVIRONMENTAL MICROBIOLOGY, Jan. 2004, p. 569–580 Vol. 70, No. 1
0099-2240/04/$08.00+0 DOI: 10.1128/AEM.70.1.569–580.2004

Microstructural Characterization of Cyanobacterial Mats from the McMurdo Ice Shelf, Antarctica

Asunción de los Ríos,[1]* Carmen Ascaso,[1] Jacek Wierzchos,[2] Eduardo Fernández-Valiente,[3] and Antonio Quesada[3]

Centro de Ciencias Medioambientales, CSIC, 28006 Madrid,[1] Servei de Microscopía Electrónica, Universitat de Lleida, 25198 Lleida,[2] and Departamento de Biología, Universidad Autónoma de Madrid, 28049 Madrid,[3] Spain

Received 30 June 2003/Accepted 25 September 2003

The three-dimensional structures of two types of cyanobacterium-dominated microbial mats from meltwater ponds on the McMurdo Ice Shelf were as determined by using a broad suite of complementary techniques, including optical and fluorescence microscopy, confocal scanning laser microscopy, scanning electron microscopy with back-scattered electron-imaging mode, low-temperature scanning electron microscopy, and microanalyitical X-ray energy dispersive spectroscopy. By using a combination of the different in situ microscopic techniques, the Antarctic microbial mats were found to be structures with vertical stratification of groups of cyanobacteria and mineral sediments, high contents of extracellular polymeric substances, and large void spaces occupied by water. In cyanobacterium-rich layers, heterocystous nostocalean and nonheterocystous oscillatorialean taxa were the most abundant taxa and appeared to be intermixed with fine-size deposits of epicellular silica and calcium carbonate. Most of the cyanobacterial filaments had similar orientations in zones without sediment particles, but thin filaments were tangled among thicker filaments. The combination of the microscopic techniques used showed the relative positions of biological and mineral entities within the microbial mats and enabled some speculation about their interactions.

Microbial mats are multilayer microbial communities whose gross morphology is determined by the dominant species of cyanobacterium, the sediments, and environmental factors (33, 36). The gliding motility of filamentous cyanobacteria in conjunction with copious excretion of extracellular polysaccharide sheath material enables these organisms to spread out on different sediments (17). Cyanobacterial mats are found in a broad range of environments (27). In the Arctic and Antarctic regions these communities are widespread in lakes, ponds, streams, glaciers, and ice shelves, and they often dominate the total biomass and biological productivity due to their adaptation to the polar environment (38).

Microscopy has always been essential for studying the morphology of microbial mats, and light microscopy has been the mainstay of such research (36). Scanning electron microscopy has been fundamentally important for analyzing mat structure from the early studies on (5, 6, 7, 11, 21, 31, 40),but this technique has provided little ultrastructural detail other than that which is apparent externally (35). The development by Wierzchos and Ascaso (41) of a method to study the microorganism-lithic substrate interface by scanning electron microscopy in back-scattered electron-imaging mode (SEM-BSE) increased the possibility of using scanning electron microscopy to study microbial communities at interfaces. New insights have also been derived from the application of novel microscopic methods to these systems, including low-temperature electron microscopy (LTSEM) and confocal laser scanning microscopy (CLSM). These new technologies have shown that microbial mats are more dynamic and structured than previously thought (4, 26, 43).

The interpretation of microbial mats as functionally integrated microbial consortium systems (27) makes integrated analysis of all the components and the way in which the different components are organized extremely interesting. Hence, the aim of this work was to study the structures of Antarctic microbial mats from two different ponds in the McMurdo Ice Shelf by analyzing which microorganisms were present throughout the mats and their contributions to the structures. The method used for this analysis was a combination of different microscopy techniques, including optical and fluorescence microscopy, CSLM, SEM-BSE, LTSEM, and microanalytical X-ray energy dispersive spectroscopy (EDS).

MATERIALS AND METHODS

Site description. The samples were collected in January 2000 in the McMurdo Ice Shelf ablation zone close to Bratina Island (78°00′S, 165°35′E). The McMurdo Ice Shelf ablation zone is a 1,500-km^2 expanse of marine-derived ice floating on the sea and is covered by numerous meltwater ponds and streams. These ponds are colonized by thick, cyanobacterium-dominated mats (39). Two types of mats from two different ponds were sampled in the present study; these ponds were Casten Pond and Black Dot Pond, which had typical conductivities of 291 and 2,260 μS cm^{-1}, respectively, and were located about 500 m from each other. The ponds in this area are typically considered N limited with relatively high dissolved reactive phosphorus and low dissolved inorganic nitrogen concentrations (18), which result in consistently low dissolved reactive phosphorus/dissolved inorganic nitrogen ratios (typically <1) (12). Both ponds were colonized by cyanobacterial mats, which completely covered the bottom surface of each pond. The environmental conditions endured by the mats in the area have been described previously (19).

Sample manipulation. Samples were collected from different sides of each pond at a depth of about 15 cm by cutting squares (3 by 3 cm) of the cohesive layer and placing them on a plastic tray with a plastic spatula. Then several cores were taken with a metal corer with an inside diameter of 11 mm. After the excess water was removed by placing the cores on absorbent paper for 30 s, the cores were placed on dry absorbent paper and stored in sterile plastic bags in a freezer.

* Corresponding author. Mailing address: Centro de Ciencias Medioambientales, C/ Serrano 115 duplicado, 28006 Madrid, Spain. Phone: 34-917452500. Fax: 34-915640800. E-mail: arios@ccma.csic.es.

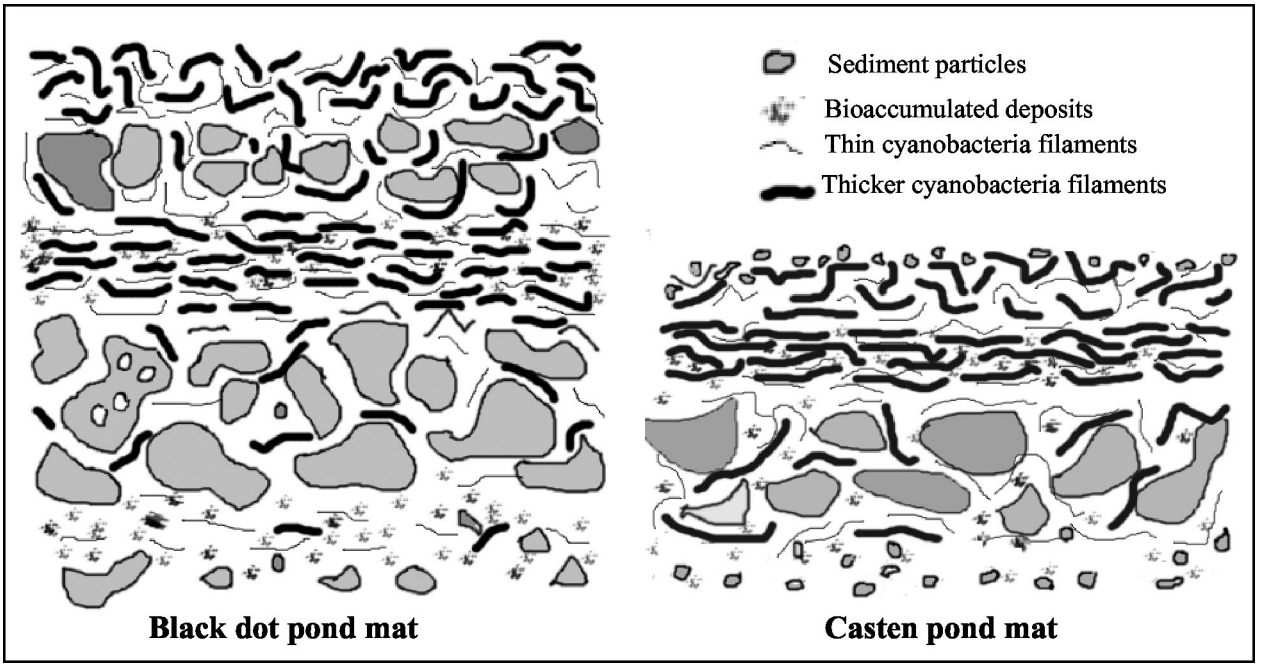

FIG. 1. Two-dimensional diagram of microbial mat structures. The thick lines represent the thicker cyanobacterial filaments (*Oscillatoriales* and *Nostocales*), and the thin lines represent *Leptolyngbya*. The filaments are drawn parallel to the surface in order to simplify the diagram, but filaments are also oriented perpendicular to the surface. The drawings are not to scale in order to show the structural differences between the mats.

The frozen samples were stored in the laboratory at −80°C until taxonomic, microscopic, and microanalytical analyses were carried out. Several cores from each mat (3–5) were prepared and sectioned for the different microscopic analyses. Some of the cores were not frozen but were teased out and examined at the site by light and epifluorescence microscopy.

Optical and fluorescence microscopy of fresh samples. In the laboratory, the frozen material was cut with a razor blade into several thick sections (thickness, >100 μm) for epifluorescence observation under low magnification (×40) to examine the distribution of the cyanobacterial cells within a mat. Green light excitation was used to obtain phycobiliprotein fluorescence that was intense red and orange (from emission by phycocyanin and phycoerythrin, respectively), which was primarily due to cyanobacteria in the environments. Other sections of the cores were teased out and examined by bright-field microscopy under higher magnification (×400 to ×1,000). Both types of observations were done with an Olympus BH-2 microscope, and the images were recorded with a Leica DC300F digital camera at resolutions of 1950 × 1545 and 1300 × 1030 pixels for the low and high magnifications, respectively.

Sample preparation for optical microscopy and CSLM. Samples were prepared by a procedure based on glutaraldehyde-induced fluorescence of plant tissues (42). In brief, samples of the mats were first fixed in glutaraldehyde (3% in 0.1 M sodium phosphate buffer [pH 7.1]), dehydrated in a series of ethanol solutions, and embedded in LR-White resin. Blocks of resin-embedded mat samples were transversely cut into two parts, and both parts of each block were finely polished.

Sample preparation for scanning electron microscopy and EDS. Samples were prepared by the procedure developed for observing the rock-microorganism interface by SEM-BSE 41). This procedure is similar to the procedure described above for CLSM, but there was osmium tetroxide fixation (1% in 50 mM sodium phosphate buffer [pH 7.1]) after glutaraldehyde fixation.

CSLM. Polished transverse sections of an embedded mat were used for examination with LSM 310 Zeiss confocal and Bio-Rad MRC 1024 microscopes. An argon laser was used to generate an excitation wavelength of 488 nm, and the resultant emission was filtered through a long-pass filter (wavelength, > 515 nm). The three-dimensional images were made up of several confocal sections at 0.5- to 1-μm increments through the sample by computer-assisted microscopy. Three-dimensional reconstruction was used for visualization of each mat's three-dimensional structure.

SEM-BSE and EDS. Polished transverse sections of an embedded mat were carbon coated and examined with DSM 940 A Zeiss and DSM 960 A Zeiss microscopes (both equipped with a four-diode semiconductor BSE detector and a Link ISIS microanalytical EDS system). SEM-BSE examination and EDS examination of the samples were performed simultaneously. Each microscope was operated at an acceleration potential of 15 kV and a specimen current of 1 to 5 nA.

LTSEM. Untreated samples of mats were examined by using the LTSEM technique. Small fragments were mechanically fixed onto the specimen holder of a cryotransfer system (Oxford CT1500), plunged into subcooled liquid nitrogen, and then transferred to a preparation unit via an air lock transfer device. The frozen specimens were cryofractured and transferred directly via a second air lock to the microscope cold stage, where they were etched for 2 min at −90°C. After ice sublimation, the etched surfaces were sputter coated with gold in the preparation unit. Samples were subsequently transferred onto the cold stage of the scanning electron microscope chamber. Fractured surfaces were observed with a DSM 960 Zeiss scanning electron microscope at −135°C under the following conditions: acceleration potential, 15 kV; working distance, 10 mm; and probe current, 5 to 10 nA.

RESULTS

The mats observed by optical microscopy were clearly distinctive; while the Black Dot Pond mat was about 3 mm thick, the Casten Pond mat was on average 0.84 mm thick. Different structures were also observed for samples from the two ponds, as shown in Fig. 1. The microbial mats from the Black Dot and Casten ponds were determined by SEM-BSE (Fig. 2A and B) and optical microscopy (Fig. 2C) to be morphologically diverse microbial communities intimately associated with mineral particles. The Black Dot mat microstructure (Fig. 2A) showed that the largest sediment particles were present at the bottom of the mat; moreover, several other layers of smaller mineral particles were present between layers of cells (Fig. 1). At the surface mineral grains were found to be loosely surrounded by biological material. However, the Casten Pond mat microstructure (Fig. 2B to D) was less complex, with only a layer of

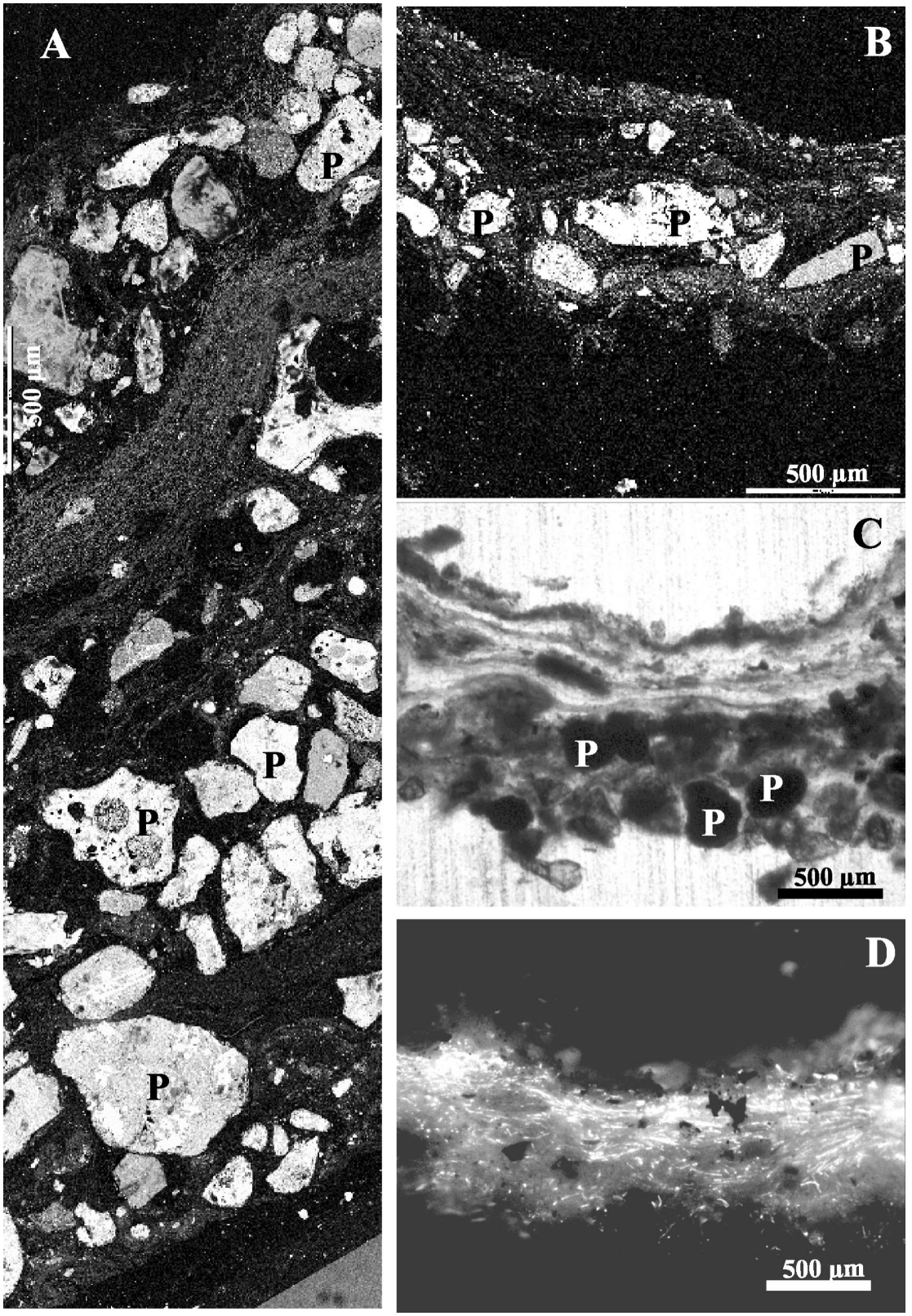

FIG. 2. General view of microbial mats from the McMurdo Ice Shelf: SEM-BSE micrographs showing transverse sections of microbial mats from Black Dot Pond (A) and Casten Pond (B) and optical micrographs of microbial mats from Casten Pond in transmission light mode (C) and in fluorescence mode (D). P, mineral particle.

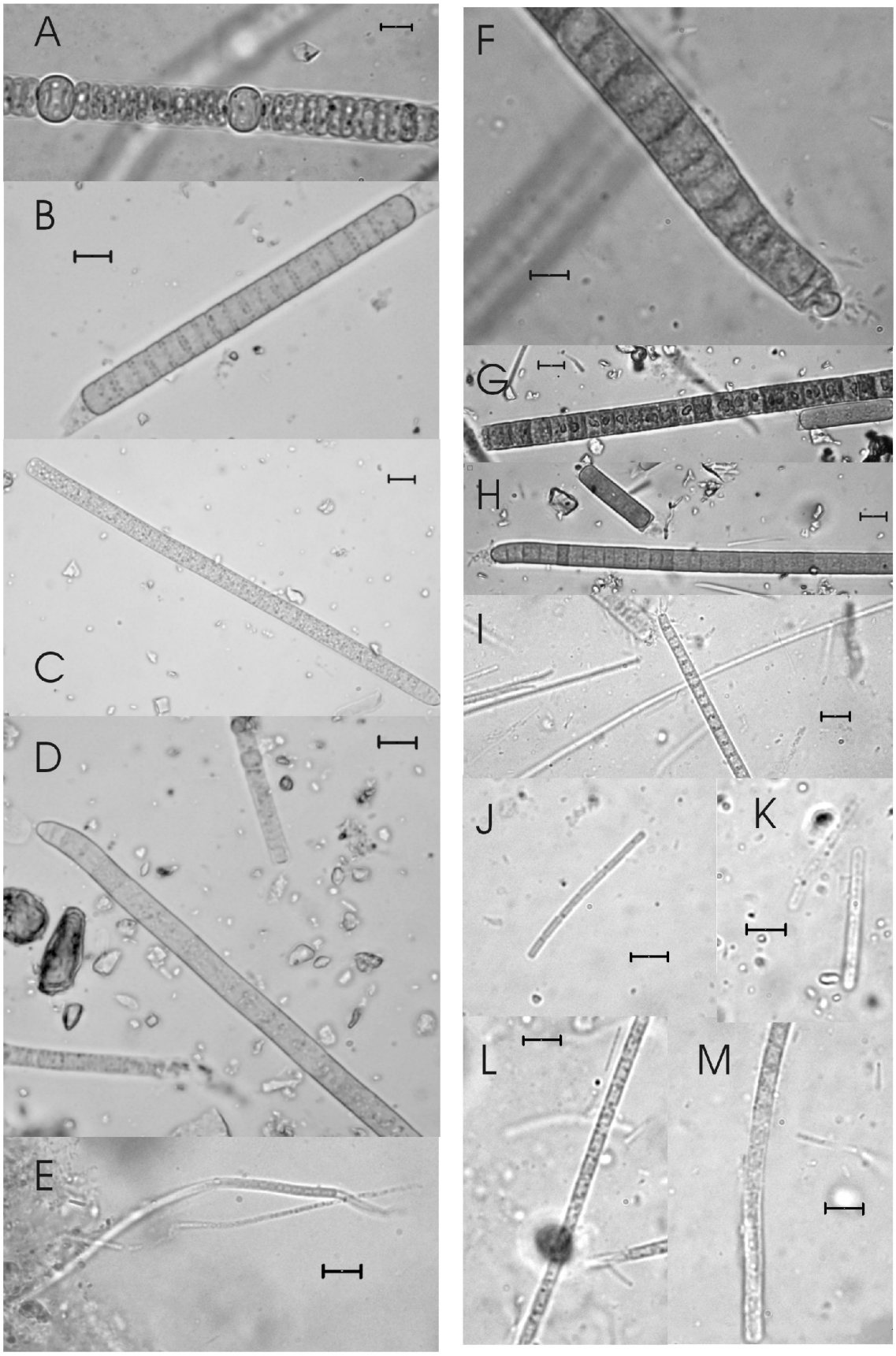
A
B
C
D
E
F
G
H
I
J
K
L
M

mineral particles located at the bottom of the mat (Fig. 1). Vertical stratification of groups of microorganisms and mineral sediments was observed. Cyanobacteria formed the intermediate layers of the mat, but differences in thickness and structure were observed in samples from both ponds. The cyanobacterial biomass in the Black Dot mat, as shown by fluorescence microscopy, occurred mainly in the top half of the mat profile, and although some cyanobacterial filaments were found to be associated with mineral particles in the bottom half, this layer was almost devoid of cyanobacteria (data not shown). The Casten Pond mat had only one cyanobacterium-rich layer (Fig. 2D), although thin layers of cyanobacteria surrounded most of the mineral material.

The mats harbored a variety of morphologically recognizable microorganisms, although cyanobacterial taxa were the most abundant organisms and constituted the majority of the biomass. Some diatoms and green algae were also found, although they did not contribute significantly to the biomass. The Casten Pond mat was formed mainly by members of the *Oscillatoriales* of different sizes (Fig. 3B to E). Two species of thin filamentous cyanobacteria, probably organisms assigned to the genus *Leptolyngbya*, which were 0.7 and 1.3 μm in diameter, were present and formed the matrix of the mat. A continuous gradient of cyanobacterial filament diameters from 3 to 9 μm was found in this mat. However, the most abundant classes were the morphotype C class (diameter, 5.4 to 6.4 μm) and the morphotype D class (diameter, 6.9 to 8.2 μm), as described in the analysis of Broady and Kibblewhite (3) of oscillatorialean diversity in this region of Antarctica. Most of the cyanobacteria found had aerotopes and other cytoplasmatic inclusions. Heterocystous cyanobacteria were also represented in this mat; these organisms included some members of the genus *Anabaena* and a conspicuous population of *Nodularia* sp. (cells that were 4.8 μm in diameter and 2.2 μm long) (Fig. 3A). The mat from Black Dot Pond was more diverse than the Casten Pond mat. Heterocystous cyanobacteria were less abundant, but large members of the *Oscillatoriales* were more abundant and diverse. Up to 13 different sizes were distinguished, ranging from 3.3 to 9.9 μm in diameter. However, when the size morphotypes suggested by Broady and Kibblewhite (3) were used, most of the cells belonged to morphotypes B (diameter, 3.6 to 5.4 μm), D (diameter, 6.9 to 8.2 μm), and E (diameter, 8.2 to 10.9 μm) (Fig. 3F to I). Thin cyanobacteria also had very diverse cell sizes, ranging from 0.6 to 2 μm in diameter (Fig. 3J to M); some of the cells were isodiametric (1.4 by 1.6 μm), and other cells were clearly elongated (1.3 by 3 μm). Several genera in this group, including *Leptolyngbya* and *Pseudanabaena*, were probably represented. Diatom frustules, as well as colonial green algae, were also found.

LTSEM examination of the pond mats revealed populations of filamentous cyanobacteria (Fig. 4A) trapped among extracellular polymeric substances (EPS) and mineral deposits. EPS located at and outside the cyanobacterial cell surface (Fig. 4B) were clearly visualized by this technique. By using LTSEM samples were examined frozen, and microorganisms may have been observed in their natural state of hydration and native position. We aimed to use a cryofixation process that was fast enough to avoid crystal formation, and the lack of chemical fixation permitted observation of the cells and EPS in conditions close to natural conditions. Some of the cells were circular in transverse section, while others were more star-like (Fig. 4B and C). Some ultrastructural details of cells could be determined from the study of cryosectioned cells (Fig. 4B and D). The cyanobacterial cells appeared to be occupied by thylakoids (Fig. 4D) and diverse granules (Fig. 4D). Cyanobacteria belonging to the different groups described above were recognized on the basis of size and morphology; these groups included *Nodularia* sp. (Fig. 4C) and the narrow filaments of *Leptolyngbya* sp. (Fig. 4B and C). Some eukaryotic algae were also observed in these mats. A colony of green algae was visualized (Fig. 4E) and was also identified by comparing the emission with blue and green light excitation in the epifluorescence microscope. Figure 4F shows a diatom frustule trapped among EPS and in the proximity of a cyanobacterial filament. The technique also permitted us to analyze the localization of water in the mats. Water occupied the spaces between cells and mineral particles and was distributed homogeneously throughout the mats (Fig. 4A). Zones with a higher capacity for water retention were not distinguished.

The structure of each mat and the ultrastructure of the cells were analyzed better by SEM-BSE at room temperature. Cyanobacteria belonging to the different groups described above were observed intermixed in different layers in the Black Dot mat (Fig. 5A). Heterocystous *Nodularia* cells were identified in the proximity of other nonheterocystous forms having the morphotypes described above, such as *Phormidium* and *Leptolyngbya* cells (Fig. 5B to D). Filamentous cyanobacterial cells without a clear orientation were present at the top of the Black Dot mat (Fig. 1 and 5B and C). However, in the cyanobacterial layer localized under the most superficial sediment layer, fila-

FIG. 3. Optical micrographs of the cyanobacteria found in the two microbial mats which were investigated. (A to E) Morphotypes found in the Casten Pond mat. (A) *Nodularia* sp. Magnification, ×1,000. Scale bar = 5 μm. (B) Oscillatorian about 9 μm in diameter belonging to the D morphotype (see text), classified classically as *Phormidium autumnale*. Scale bar = 10 μm. (C) Cyanobacterium about 7 μm in diameter belonging to the C morphotype, also considered *P. autumnale*. Scale bar = 10 μm. (D) Oscillatorian 6.7 μm in diameter, showing the typical bending at the end of trichome. This organism also belongs to the D morphotype. Scale bar = 10 μm. (E) Two thin cyanobacteria 0.7 and 1.3 μm in diameter, probably belonging to the genus *Leptolyngbya*. Scale bar = 10 μm. (F to L) Some of the morphotypes found in the Black Dot Pond mat. (F) Detail of the calyptra, one of the taxonomic aspects considered in classification of the *Oscillatoriales*. This organism belongs to the E morphotype. Scale bar = 5 μm. (G) Another morphotype E oscillatorian, which is 8.9 μm in diameter and has large granules inside the cells. Scale bar = 10 μm. (H) A 7.1-μm-wide oscillatorian belonging to morphotype D, with bacteria attached to the end of the filament. Scale bar = 10 μm. (I) Smaller cyanobacterium which is 4 μm in diameter and belongs to morphotype B. Scale bar = 10 μm. All the organisms shown in panels F to I are included in the species *P. autumnale*. (J to M) Organisms less than 2 μm in diameter. (J) Organism about 0.6 μm in diamter. Scale bar = 5 μm. (K) Organism about 1 μm in diameter. Scale bar = 5 μm. (L) Organism 1.4 μm in diameter. Scale bar = 5 μm. (M) Organism 2 μm in diameter. Scale bar = 5 μm.

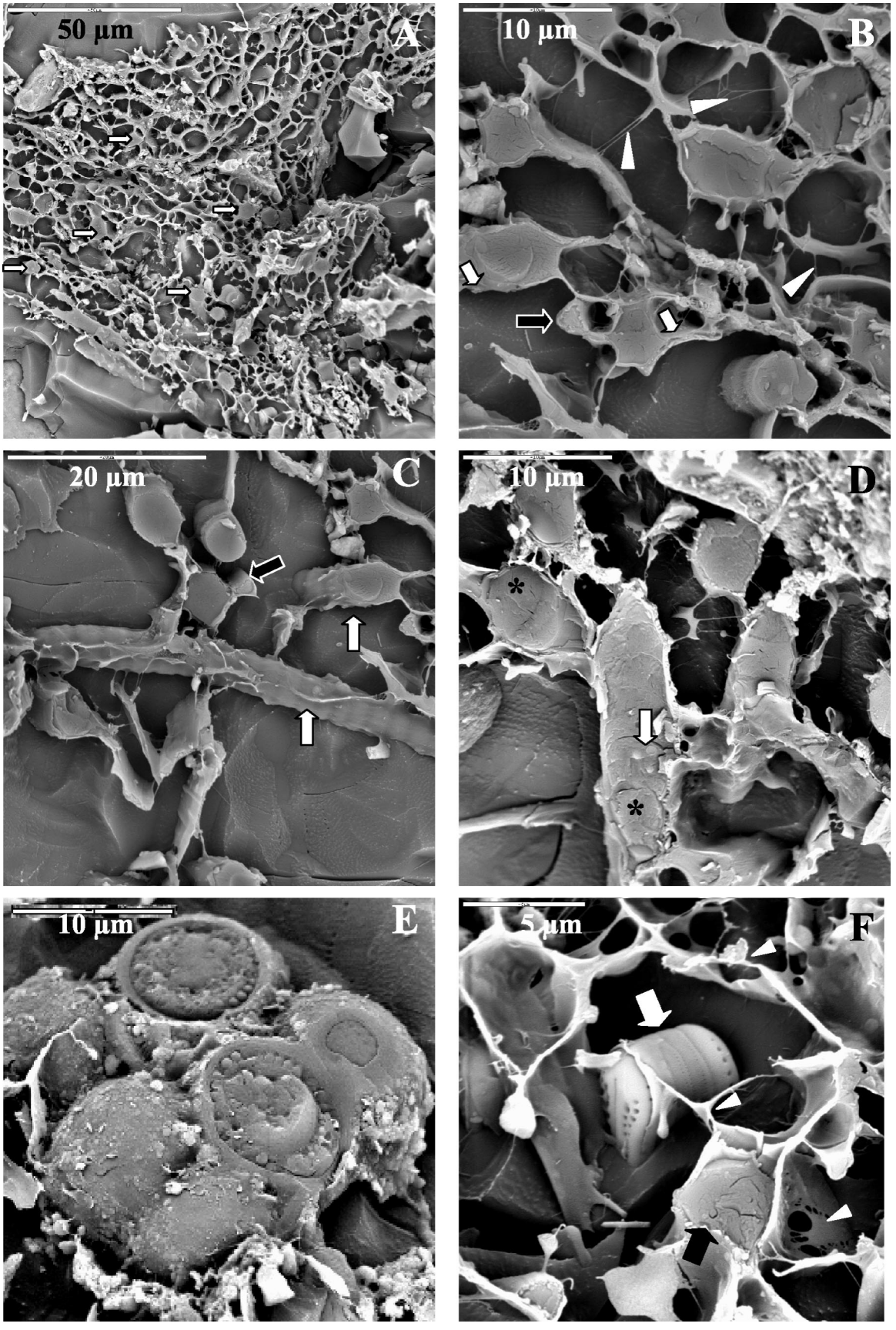
50 µm
A
10 µm
B
20 µm
C
10 µm
D
10 µm
E
5 µm
F

mentous cyanobacteria had an orientation parallel to the surface and also to each other (Fig. 1 and 5D). Some cyanobacterial cells were also observed deeper in the mat, but generally these cells were scarce and associated with sediments. The cyanobacterium-rich layer was localized in the Casten mat under the thin layer of small mineral deposits present at the top of the mat (Fig. 1 and 5E). At the bottom of the cyanobacterium-rich layer, thin filamentous cyanobacteria likely belonging to the genus *Leptolyngbya*, diatoms, and bacteria were frequently observed (Fig. 5F).

SEM-BSE observation of several cross sections of Antarctic microbial mats revealed the presence of different mineral phases within the mats. Accumulations of small mineral particles and diatom frustules (Fig. 6A) were observed in the bottoms of mats in the proximity of some filamentous cyanobacteria (Fig. 6A). These particles were chemically heterogeneous, as shown by the EDS elemental distribution map (Fig. 6B). Fine-size mineral deposits were frequently observed among forms of filamentous cyanobacteria present in the cyanobacterium-rich layers of both mats (Fig. 5F and 6C and D). The nature of these mineral deposits was analyzed by the EDS microanalytical technique. Figures 6E to G show the EDS elemental distribution maps for silicium (Si), calcium (Ca), and aluminum (Al) in different zones of the Black Dot Pond and Casten Pond mats. The data revealed the presence of weakly laminated silica layers associated with aluminum (Fig. 6F). These siliceous deposits appeared to accumulate in certain areas of the mats (Fig. 6D, F, and G) or in thin bands among filamentous cyanobacteria (Fig. 6C and E). These mineral deposits were also observed, intermixed with partially decomposed cells, in the layers without sediments localized in the bottom of the Black Dot mat. Bioaccumulations of calcium, as revealed by EDS elemental distribution maps, are shown in Fig. 6E and G; these deposits corresponded to the fine crystalline calcium carbonate deposits formed in situ (Fig. 5A). Both kinds of deposits were present in both mats and were always associated with the presence of filamentous cyanobacteria. Epicellular silica gel and calcium carbonate deposits were not observed in zones close to the surface. Allochthonous particles of clay minerals without signs of bioalteration were located in the sediment layers (Fig. 5E).

The nature and the spatial organization of the mats were further analyzed by confocal microscopy. Stereoimages confirmed the filamentous nature of the majority of the cells (Fig. 7A). Cyanobacterial filaments had similar orientations in zones without big mineral particles (Fig. 7B), although the thin filaments were tangled among the thicker filaments. Particles were densely covered by filamentous cyanobacterial forms, which were randomly oriented in their proximity (Fig. 7C). Cyanobacteria that were different sizes and had different morphologies were spatially intermixed in some zones (Fig. 7D), exhibiting a close relationship (Fig. 7E). Bacterium-like cells were also recognized by this technique in the proximity of cyanobacterial filaments (Fig. 7F).

DISCUSSION

The cyanobacterial mats from the Casten and Black Dot ponds can be considered representative of the mats in the area where they were collected; however, much thicker mats and other morphologies are also found in the area (39). The mats which we studied were composed of mixtures of different species organized in different layers, and there was alternation of layers composed basically of mineral sediments and layers composed of filamentous cyanobacteria mixed with small mineral deposits. This complexity implied that it was necessary to combine different microscopy techniques to identify all the components and the relationships among them. The techniques used here permitted us to analyze in situ the different components of the mats, both organic and inorganic, without apparently disturbing the organization of the mats. The living and nonliving forms of cyanobacteria identified by optical and fluorescence microscopy could be characterized ultrastructurally in situ by SEM-BSE. This is extremely important because it was difficult to obtain these details by other techniques, such as transmission electron microscopy; the sectioning of the microbial mats necessary for transmission electron microscopy was difficult due to the presence of mineral particles (11). The combination of SEM-BSE with an analytical X-ray EDS system permitted detailed analysis of the localization of the inorganic compounds. The LTSEM technique provided the most realistic mat structure since it allowed complete examination of the mat without invasive treatments. Finally, CLSM gave a detailed view of the three-dimensional microstructure of the mat.

This combination of diverse microscopy techniques showed that the Antarctic microbial mats studied are open structures containing a high fraction of EPS and large void spaces occupied by water. The EPS were found to be closely related to cyanobacteria and eukaryotic algae. We do not completely understand which environmental conditions regulate the excretion of EPS by microorganisms or what the exact function of the EPS in the mat is. However, the extracellular microbial compounds produced by the different groups of microorganisms present in the mats studied seem to be involved in attachment of microorganisms to the substrate and in the formation of a matrix in which the microorganisms are embedded (8, 9, 33). On the other hand, thin cyanobacterial filaments (mainly *Leptolyngbya* sp.) form a dense network among the sediments and also among the rest of cyanobacteria. EPS and the thin filamentous cyanobacterial network could constitute the main forces that stabilize and provide cohesion for the microbial mats. This cohesion is essential to prevent lifting of the mats by

FIG. 4. LTSEM of microbial mats from the McMurdo Ice Shelf. (A) General view of Casten Pond microbial mat zone with numerous filamentous cyanobacteria (arrows). (B) Transversely sectioned filamentous cyanobacteria. EPS at the cell surface are indicated by white arrows, and the EPS that have been released and are located outside the cell are indicated by arrowheads. The black arrow indicates a *Leptolyngbya* filament. (C) Sectioned and nonsectioned *Nodularia* (white arrows) and *Leptolyngbya* (black arrow) filamentous cells immersed in frozen water. (D) Transverse and longitudinal sections of filamentous cyanobacteria showing several ultrastructural details. The asterisks indicate thylakoids, and the arrow indicates cytoplasmic granules. (E) Colony of unidentified green algae. (F) Diatom frustule (white arrow) and filamentous cyanobacteria (black arrow) surrounded by EPS (arrowheads).

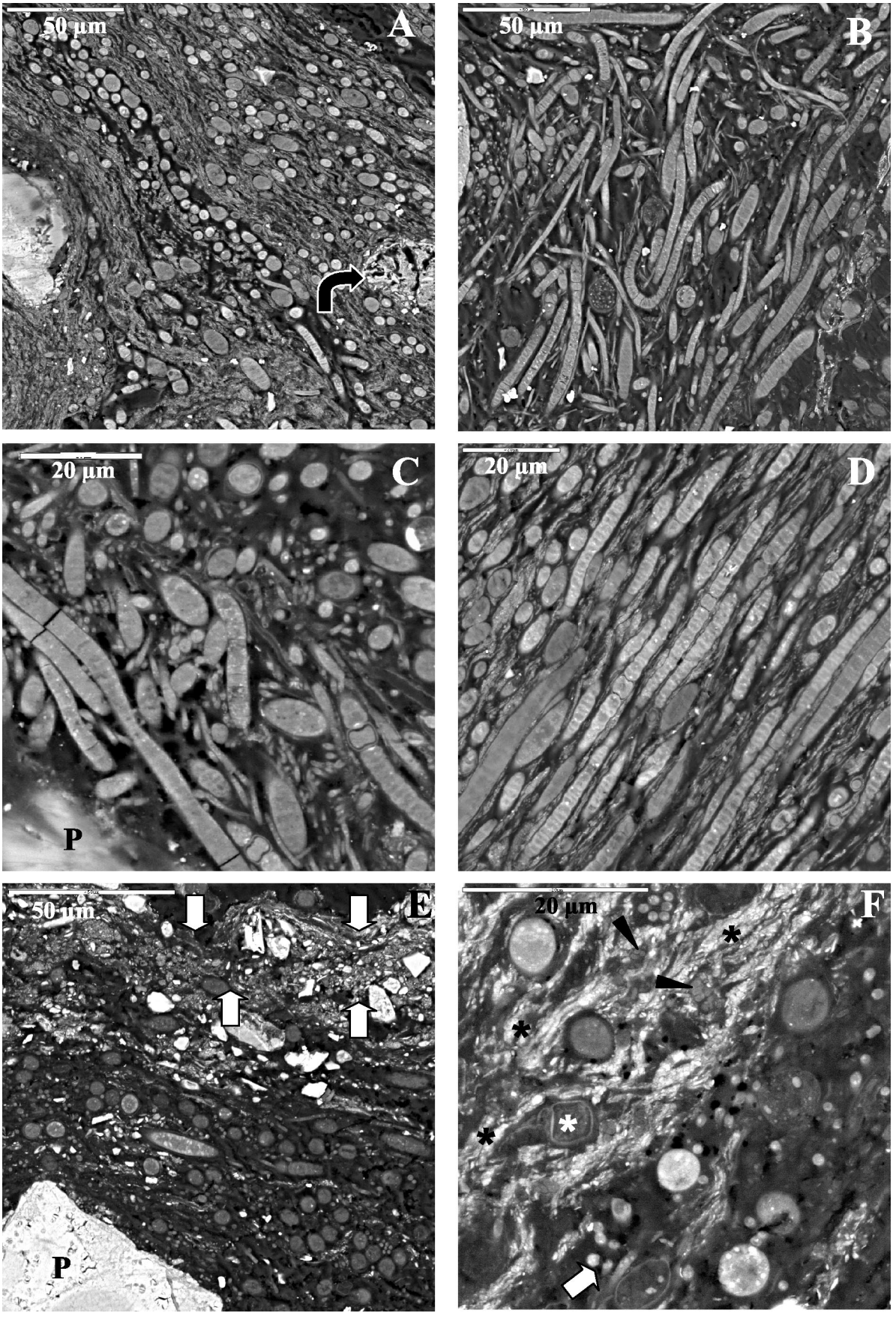
50 μm
A
50 μm
B
20 μm
C
P
20 μm
D
50 μm
E
P
20 μm
F

ice working and wind stress. The structures of these Antarctic microbial mats can be closely related to the interactions and activities that occur in the communities (37). The void spaces, which were observed by LTSEM and CLSM, can play important ecological roles in the functioning of stratified structures, such as these microbial mats. Cell-free channels and pores increase the influx of liquid and nutrients to the inner parts of mats and facilitate the efflux of wastes (37). Also, void spaces could permit the gliding movements and changes in orientation of filamentous cyanobacteria that have been observed in some microbial mats, including mats from the McMurdo Ice Shelf (2, 15, 24, 31). Heterocystous and nonheterocystous cyanobacterial taxa were found to be intermixed in the microbial mats studied, although filamentous nonheterocystous taxa were the dominant organisms. Nonheterocystous cyanobacteria are versatile organisms that can cope well with the fluctuating physical conditions of a mat, while heterocystous cyanobacteria are well suited for contemporaneous nitrogen fixation and oxygenic photosynthesis (34). The presence of heterocystous forms suggests that N_2 fixation plays an important role in the nitrogen economy of these ecosystems, as has been demonstrated in other mats from the same area (12, 30), although the possibility of N_2 fixation by nonheterocystous cyanobacteria cannot be excluded. It appeared that there was not any obvious spatial distribution of heterocystous forms throughout the mats, although in a multilayer mat with different oxygen concentrations in the mat profile ubiquity is expected since the heterocysts may represent an effective defense against oxygen for the nitrogenase system.

The in situ characterization of organic and inorganic mat compounds by the combination of SEM-BSE and EDS provided more precise information concerning the mat microstructure. The structural details obtained are well integrated in the three-dimensional organization supported by the results of CSLM and LTSEM. Close spatial relationships not only between different cyanobacterial filaments but also between filaments and sediment particles could be established. Biological stratification has been observed to be associated with biomineralogical stratification (23) which results in the formation of different microenvironments in a mat. Weakly laminated silica layers among filamentous cyanobacteria were observed in both mats. These finely laminated siliceous sinters were composed of a heterogeneously nucleated amorphous silica matrix which seemed to precipitate in the spaces between filaments. This observation indicates that biologically active microbial communities could facilitate silicification, probably by providing reactive interfaces for silica adsorption, thereby reducing the activation energy barriers to nucleation and permitting surface chemical interaction that sorbs more silica from solution. Biogenically formed silica has also been observed in Antarctic endolithic microorganisms (1). The sources of silica in cyanobacterial mats could be the allochthonous aluminosilicate clay minerals, as well diatom frustules. Cyanobacterial cells with their EPS may merely act as reactive interfaces or templates for heterogeneous nucleation (13, 20, 22, 32). After this nucleation, silica precipitation could presumably continue autocatalytically and abiogenically due to the increase in surface area generated by the small silica phases (22). The presence of calcium carbonate closely associated with cyanobacterial cells indicated that the cells may participate in the formation of this biomineral. Calcification is a common phenomenon in microbial mats and seems to be influenced and controlled by the microorganisms present in a mat (11, 33). On the other hand, the chemically heterogeneous deposits observed in the microbial mats could have originated from aeolian contamination and/or from suspension in flowing water. It is known that cyanobacterial mats promote sediment accretion by selectively incorporating sediment particles which would otherwise be swept away by current and wind (17). It has been demonstrated that mat-forming microorganisms can produce sticky excretions that are able to trap allochthonous mineral grains within the mats (16). The interplay between physical and chemical factors around sediment particles can create zones where the growth and proliferation of certain species are promoted (9, 36). During some periods the darker particles may absorb sufficient solar energy to cause localized heating and melting in a frozen mat, which would favor biological activity and hence the creation of different microenvironments (14, 25). The presence of such sediment particles could thus influence the formation of certain gradients and microenvironments within mats. The microbial mat structure observed here is likely to facilitate the life of the cyanobacteria under the harsh Antarctic conditions. Association of functionally diverse microorganisms in structured habitats seems to be an effective strategy for meeting the requirements of life in one of the most extreme environments on earth (10, 28). The two mats investigated here differed in terms of thickness and number of layers, and the differences were probably related to different ages of the mats (the Black Dot Pond mat was probably older than the Casten Pond mat). Microbial mat growth is frequently caused by accumulation of empty cyanobacterial sheaths and mineral deposition (11, 29). The different layers observed in the Black Dot mat could represent different growth phases of the mat. The loose upper layers of upright filaments in the mat represent recent growth layers. Overgrowth of the younger filaments and sediment accretion may have compacted the layers (26). The layers composed of the rest of the cyanobacterial cells and fine silica mineral fragments could be zones occupied previously by cyanobacterial cells.

The microscopic and microanalytical techniques used here

FIG. 5. SEM-BSE micrographs of Black Dot Pond (A to D) and Casten Pond (E and F) mats. (A) General view of cyanobacterium-rich layer. The arrow indicates a calcium carbonate precipitate. (B) General view of the upper part of the mat. (C) *Nodularia*, *Leptolyngbya*, and *Phormidium* intermixed in the proximity of a sediment particle (P). (D) Heterocystous *Nodularia* and *Phormidium* cells oriented parallel to the surface and intermixed with bands of small mineral grains. (E) General view of the upper half of the mat. The arrows indicate a thin layer of small mineral deposits at the top of the mat. P, sediment particle. (F) Transverse section of thick filamentous cyanobacteria, *Leptolyngbya* filaments (white arrow), diatoms (white asterisk), and bacteria (arrowheads) immersed in an accumulation of fine mineral deposits (black asterisks) localized in the bottom part of the cyanobacterium-rich layer.

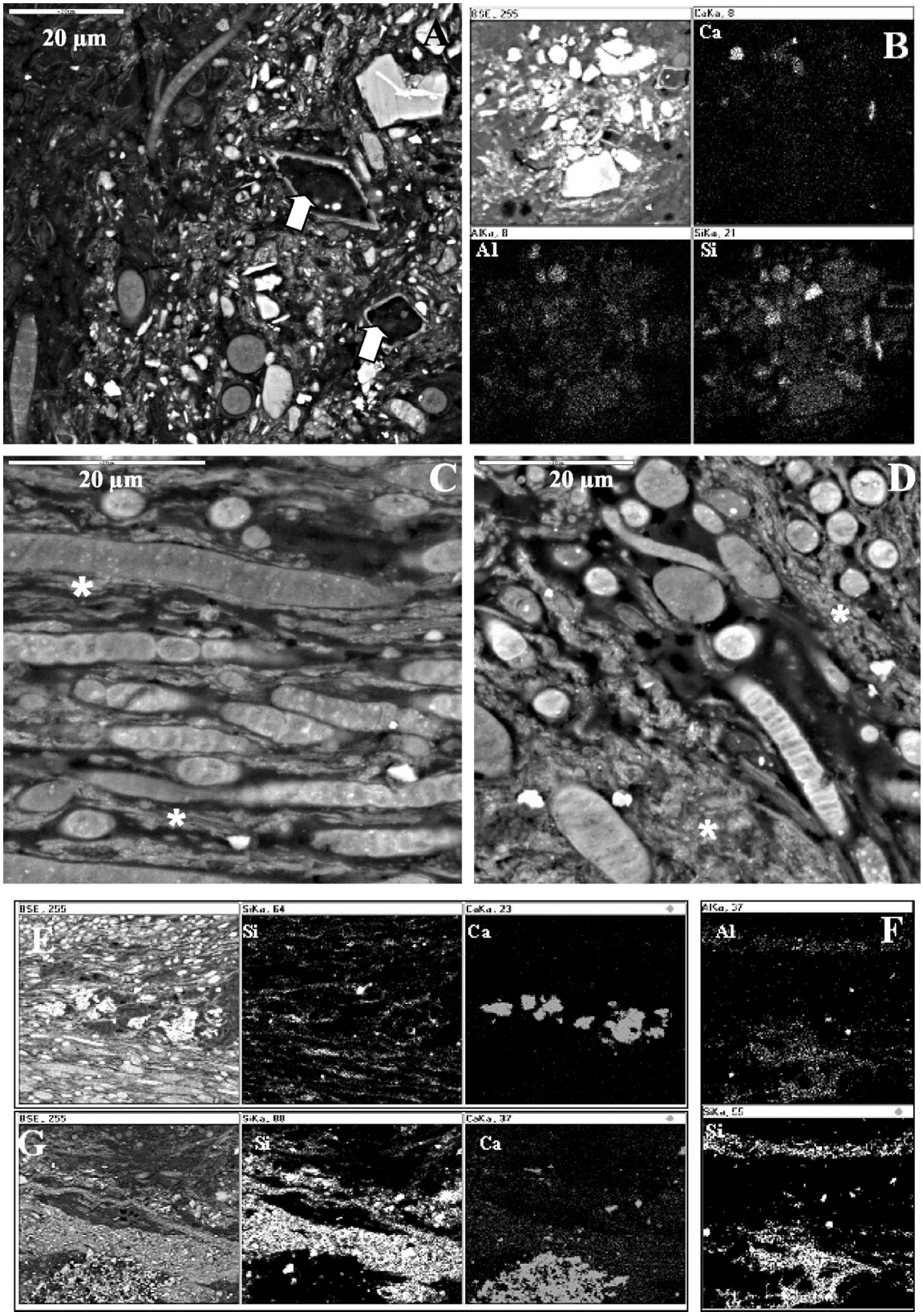

FIG. 6. SEM-BSE and EDS elemental distribution maps of bioaccumulated and allochthonous inorganic deposits within Casten Pond (A, B, and G) and Black Dot Pond (C to F) mats. (A) SEM-BSE image from the bottom part of the mat. The arrows indicate diatom frustules. (B) SEM-BSE image and EDS maps of Ca, Al, and Si, showing the chemical heterogeneity of allochthonous grains of minerals. (C and D) SEM-BSE images of *Nodularia*, *Leptolyngbya*, and *Phormidium* cells in the proximity of accumulations of fine mineral deposits (white asterisks) forming thin bands (C) or small areas (D). (E) SEM-BSE image and EDS maps of Si (indicating siliceous phase) and Ca (indicating calcium carbonate phase) of fine mineral deposits. (F) EDS maps of Al and Si showing the presence of silicified deposits. (G) SEM-BSE image and EDS maps of Si and Ca showing siliceous and calcium carbonate phases in the mat.

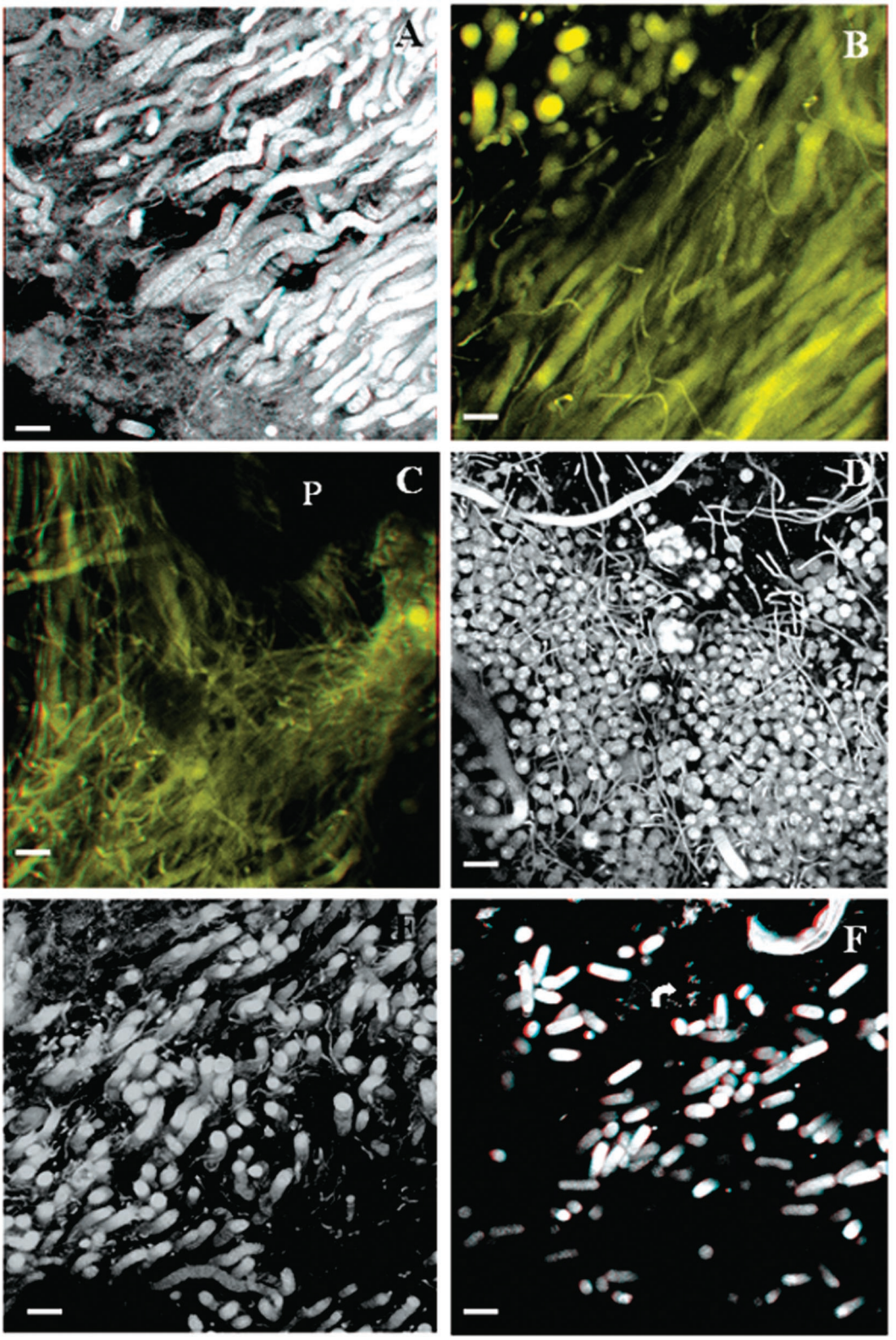

FIG. 7. Plate 7. CLSM three-dimensional images of microbial mats from the McMurdo Ice Shelf. Bars = 20 μm. The stereoimages (A, B, C, and F) can be observed by using three-dimensional color spectacles. (A) Filamentous cyanobacteria in the upper part of the Black Dot Pond mat. (B) Cyanobacterium-rich layer from the Casten Pond mat. (C) Randomly oriented cyanobacterial forms covering a sediment particle (P) from the Casten Pond mat. (D) Accumulation of randomly orientated diverse filamentous cyanobacteria from Black Dot Pond. (E) Zone occupied by cyanobacteria of different sizes, showing the close relationship among the cells. (F) Filamentous cyanobacterial cells from Casten Pond in the proximity of bacterium-like cells (arrow).

provided a complementary suite of approaches for characterizing microbial mats. Application of a single method can result in a misleading estimate of the biodiversity and a more limited appreciation of the three-dimensional organization of biogenic and nonbiogenic components within mats. Future studies will increasingly rely on molecular approaches. These approaches still need to be combined with advanced microscopy to understand the spatial relationships among individual genotypes.

ACKNOWLEDGMENTS

This work was supported by grants BOS2000-1121, REN2002-03542, ANT96-2174-E, ANT99-1319-E, and REN2000-0435-ANT.

We thank Fernando Pinto and Sara Lapole (Centro de Ciencias Medioambientales) for technical assistance, Antarctic New Zealand for logistic support and excellent field facilities, and C. Howard-Williams, I. Hawes, and R. Smith, for inviting us to participate in their Antarctic expeditions and for their help. We especially thank W. F. Vincent, I. Hawes, and C. Howard-Williams and three anonymous reviewers for their useful comments on the manuscript.

REFERENCES

1. **Ascaso, C., and J. Wierzchos.** 2003. The search for biomarkers and microbial fossils in Antarctic rock microhabitats. Geomicrobiol. J. **20:**439–450.
2. **Bebout, B. M., and F. García Pichel.** 1995. UV B-induced vertical migrations of cyanobacteria in a microbial mat. Appl. Environ. Microbiol. **61:**4215–4522.
3. **Broady, P. A., and A. L. Kibblewhite.** 1991. Morphological characterization of Oscillatoriales (Cyanobacteria) from Ross Island and Southern Victoria Land, Antarctica. Antarct. Sci. **3:**35–45.
4. **Caldwell, D. E., D. R. Korber, and J. R. Lawrence.** 1992. Imaging of bacterial cells by fluorescence exclusion using scanning confocal laser microscopy. J. Microbiol. Methods **15:**249–261.
5. **Cohen, Y., W. E. Krumbein, and M. Shilo.** 1977. Solar Lake (Sinai). 2. Distribution of photosynthetic microorganisms and primary production. Limnol. Oceanogr. **22:**609–610.
6. **Cohen, Y., and E. Rosemberg.** 1989. Microbial mats: physiological ecology of benthic microbial communities. ASM Publishing, Washington, D.C.
7. **Davey, M. C., and K. J. Clarke.** 1992. Fine structure of a terrestrial cyanobacterial mat from Antarctica. J. Phycol. **28:**199–202.
8. **Decho, A. W.** 1994. Exopolymers in microbial mats. Assessing their adaptative roles, p. 215–219. *In* L. J. Stal and P. Caumette (ed.), Microbial mats. Springer-Verlag, Berlin, Germany.
9. **Decho, A. W.** 2000. Exopolymer microdomains as a structuring agent for heterogeneity within microbial biofilms, p. 9–15. *In* R. E. Riding and S. M. Awramik (ed.), Microbial sediments. Springer-Verlag, Berlin, Germany.
10. **de los Ríos, A., J. Wierzchos, L. G. Sancho, and C. Ascaso.** 2003. Acid microenvironments in microbial biofilms of Antarctic endolithic microecosystems. Environ. Microbiol. **5:**231–237.
11. **Fenchel, T., and M. Kühl.** 2000. Artificial cyanobacterial mats: growth, structure, and vertical zonation patterns. Microb. Ecol. **40:**85–93.
12. **Fernández-Valiente, E., A. Quesada, C. Howard-Williams, and I. Hawes.** 2001. N_2-fixation in cyanobacterial mats from ponds on the McMurdo Ice Shelf, Antarctica. Microb. Ecol. **42:**338–349.
13. **Ferris, F. G., T. J. Beveridge, and W. S. Fyfe.** 1986. Iron-silica crystallite nucleation by bacteria in a geothermal sediment. Nature **320:**609–611.
14. **Fritsen, C. H., and J. C. Priscu.** 1998. Cyanobacterial assemblages in permanent ice covers on Antarctic lakes: distribution, growth rate, and temperature response of photosynthesis. J. Phycol. **34:**587–597.
15. **García-Pichel, F., M. Mechling, and R. W. Castenholz.** 1994. Diel migrations of microorganisms within a benthic, hypersaline mat community. Appl. Environ. Microbiol. **60:**1500–1511.
16. **Gerdes, G., and W. E. Krumbein.** 1987. Biolaminated deposits, p. 183. *In* S. Bhattacharya, G. M. Friedman, H. J. Neugebauer, and A. Seilacher (ed.), Lecture notes in earth sciences, vol. 9. Springer-Verlag, New York, N.Y.
17. **Golubic, S., L. Seong-Joo, and K. M. Browne.** 2000. Cyanobacteria: architects of sedimentary structures, p. 57–67. *In* R. E. Riding and S. M. Awramik (ed.), Microbial sediments. Springer-Verlag, Berlin, Germany.
18. **Hawes, I., C. Howard-Williams, and R. D. Pridmore.** 1993. Environmental control of microbial communities in the ponds of McMurdo Ice Shelf, Antarctica. Arch. Hydrobiol. **127:**271–287.
19. **Hawes, I., R. Smith, C. Howard-Williams, and A. M. Schwarz.** 1999. Environmental conditions during freezing, and response of microbial mats in ponds of the McMurdo Ice Shelf, Antarctica. Antarct. Sci. **11:**198–208.
20. **Jones, B., R. W. Renault, and M. R. Rosen.** 1998. Microbial biofacies in hot-spring sinters: a model based on Ohaaki Pool, North Island, New Zealand. J. Geol. Soc. (London) **68:**413–414.
21. **Jorgensen, B., N. P. Revsbech, and Y. Cohen.** 1983. Photosynthesis and structure of benthic microbial mats: microelectrode and SEM studies of four cyanobacterial communities. Limnol. Oceanogr. **28:**1075–1093.
22. **Konhauser, K. O., V. R. Phoenix, S. H. Bottrell, D. G. Adams, and I. M. Head.** 2001. Microbial-silica interactions in Icelandic hot spring sinter: possible analogues for some Precambrian siliceous stromatolites. Sedimentology **48:**415–433.
23. **Monty, C. L. V.** 1976. The origin and development of cryptalgal fabrics, p. 139–249. *In* M. R. Walter (ed.), Stromatolites. Elsevier, Amsterdam, The Netherlands.
24. **Nadeau, T. L., C. Howard-Williams, and R. W. Castenholz,.** 1999. Effects of solar UV and visible irradiance on photosynthesis and vertical migration of *Oscillatoria* sp. (Cyanobacteria) in an Antarctic microbial mat. Aquat. Microb. Ecol. **20:**231–239.
25. **Olson, J. B., T. F. Steppe, R. W. Litaker, and H. W. Paerl.** 1998. N_2-fixing microbial consortia associated with the ice cover of Lake Boney, Antarctica. Microb. Ecol. **36:**231–238.
26. **Oppenheim, D. R., and D. M. Paterson.** 1990. The fine structure of an algal mat from a freshwater maritime Antarctic lake. Can. J. Bot. **68:**174–183.
27. **Paerl, H. W., J. L. Pinckney, and T. F. Steppe.** 2000. Cyanobacterial-bacterial mat consortia: examining the functional unit of microbial survival and growth in extreme environments. Environ. Microbiol. **2:**11–26.
28. **Paerl, H. W., and J. C. Priscu.** 1998. Microbial phototrophic, heterotrophic, and diazotrophic activities associated with aggregates in the permanent ice cover of Lake Bonney, Antarctica. Microb. Ecol. **36:**221–230.
29. **Paterson, D. M.** 1994. Microbiological mediation of sediment structure and behaviour, p. 215–229. *In* L. J. Stal and P. Caumette (ed.), Microbial mats. Springer-Verlag, Berlin, Germany.
30. **Quesada, A., and E. Fernández-Valiente.** 2000. The role of N_2-fixation in microbial mats in Antarctic freshwater ecosystems, p. 41–46. *In* W. Davison, C. Howard-Williams, and P. Broady (ed.), Antarctic communities: species, structure and survival. New Zealand Natural Sciences, Canterbury University, Canterbury, New Zealand.
31. **Ramsing, N. B., M. J. Ferris, and D. M. Ward.** 2000. Highly ordered vertical structure of *Synechococcus* populations within the one-millimeter-thick photic zone of a hot spring cyanobacterial mat. Appl. Environ. Microbiol. **66:**1039–1049.
32. **Schultze-Lam, S., F. G. Ferris, K. O. Konhauser, and R. G. Wiese.** 1995. *In situ* silicification of an Icelandic hot spring microbial mat: implications for microfossil formation. Can. J. Earth Sci. **32:**2021–2026.
33. **Stal, L. J.** 2000. Cyanobacterial mats and stromatolites, p. 61–120. *In* B. A. Whitton and M. Potts (ed.), The ecology of cyanobacteria. Kluwer Academic Publishers, Dordrecht, The Netherlands.
34. **Stal, L. J., H. W. Paerl, B. Bebout, and M. Villbrandt.** 1994. Heterocystous versus non-heterocystous cyanobacteria in microbial mats, p. 403–414. *In* L. J. Stal and P. Caumette (ed.), Microbial mats. Springer-Verlag, Berlin, Germany.
35. **Stolz, J. F.** 1994. Light and electron microscopy in microbial mat research. An overview, p. 173–184. *In* L. J. Stal and P. Caumette (ed.), Microbial mats. Springer-Verlag, Berlin, Germany.
36. **Stolz, J. F.** 2000. Structure of microbial mats and biofilms, p. 1–8. *In* R. E. Riding and S. M. Awramik (ed.), Microbial sediment. Springer-Verlag, Berlin, Germany.
37. **Tolker-Nielsen, T., and S. Molin.** 2000. Spatial organization of microbial biofilm communities. Microb. Ecol. **40:**75–84.
38. **Vincent, W. F.** 2000. Cyanobacterial dominance in the polar regions, p. 321–340. *In* B. Whitton and M. Potts (ed.). Ecology of the Cyanobacteria: their diversity in space and time. Kluwer Academic Press, Dordrecht, The Netherlands.
39. **Vincent, W. F., M. T. Downes, R. W. Castenholz, and C. Howard-Williams.** 1993. Community structure and pigment organisation of cyanobacteria-dominated microbial mats in Antarctica. Eur. J. Phycol. **28:**213–221.
40. **Walter, M. R.** 1976. Stromatolites. Elsevier, Amsterdam, The Netherlands.
41. **Wierzchos, J., and C. Ascaso.** 1994. Application of back-scattered electron imaging to the study of the lichen rock interface. J. Microsc. **175:**54–59.
42. **Wierzchos, J., and C. Ascaso.** 2001. Life, decay and fossilisation of endolithic microorganisms from the Ross Desert, Antarctica. Polar Biol. **24:**863–868.
43. **Wiggli, M., A. Smallcombe, and R. Bachofen.** 1999. Reflectance spectroscopy and laser confocal microscopy as tools in the ecophysiological study of microbial mats in an alpine bog pond. J. Microbiol. Methods **34:**173–182.